informa
healthcare

Alkaline phosphatase inhibition by vanadyl-β-diketone complexes: electron density effects

AMANDA J. ZIEGLER, JAN FLÓRIÁN, MIGUEL A. BALLICORA, & ALBERT W. HERLINGER

Department of Chemistry, Loyola University Chicago, Chicago, IL 60626, USA

Abstract
A series of systematically modified vanadyl-β-diketone complexes, VO(β-diketone)$_2$, bearing substituent groups with different electron inductive properties were synthesized and evaluated as inhibitors against calf-intestine alkaline phosphatase (APase). A combination of biochemical and quantum mechanical techniques were employed to identify structure-activity relationships relevant for rational design of phosphatase inhibitors. Kinetic parameters and activation free energy, enthalpy, and entropy for calf-intestine APase-catalyzed dephosphorylation of *para*-nitrophenylphosphate were also determined along with the inhibition constants (K$_i$) for the VO(β-diketone)$_2$ complexes. Increased positive charge on the vanadyl group increases the inhibition potency of the complex while the absence of an available coordination site on the complex decreases its inhibition potency. These findings correlate well with the results of *ab initio* electron density calculations for the complexes.

Keywords: *Phosphatase inhibition, calf-intestine alkaline phosphatase, vanadium, vanadyl, β-diketone, electron density, inhibition*

Introduction

Alkaline phosphatases are dimeric metalloenzymes that catalyze the dephosphorylation of phosphate monoesters to inorganic phosphate and an alcohol [1,2]. The active sites of APases are generally highly conserved among species, e.g., *Escherichia coli* [2], shrimp [3], and human placenta [4]. Thus, although a crystal structure has not been reported, the active sites of calf-intestine APase are expected to be similar to the active sites of APases from other species. Calf-intestine APase is one of the most thoroughly studied phosphatases among the mammalian APases. Numerous methods have been employed in its characterization [5–8], including its inhibition by phosphate, pyrophosphate, phosphate derivatives, Mg^{2+}, Zn^{2+}, CN$^-$, F$^-$, and selected amino acids [9–11].

Vanadium compounds are known phosphatase inhibitors, for example, sodium orthovanadate is a competitive inhibitor for *E. coli* APase with a K$_i$ of 12 μM [12]. An X-ray crystal structure for *E. coli* APase with vanadate bound in both active sites reveals that vanadium's coordination geometry is trigonal bipyramidal with a serine nucleophile and coordinated water occupying the axial positions [12]. Crans and co-workers have pointed out the importance of considering vanadium's solution chemistry when using vanadium compounds as tools in biological studies [13]. An investigation of chicken-intestine APase inhibition by vanadium-dipicolinate complexes, for example, revealed that assay conditions must be controlled to obtain meaningful data [13].

Many chemical and biological studies have demonstrated the blood glucose lowering capabilities of vanadium compounds [14,15]. VO(acac)$_2$, bis(acetylacetonato)oxovanadium(IV), and VO(Meacac)$_2$, bis(3-methylacetylacetonato)oxovanadium(IV), Figure 1, as well as bis(3-ethylacetylacetonato)oxovanadium(IV) function as insulin-enhancing agents, lowering blood glucose levels of streptozocin-induced rats and

RIGHTSLINK

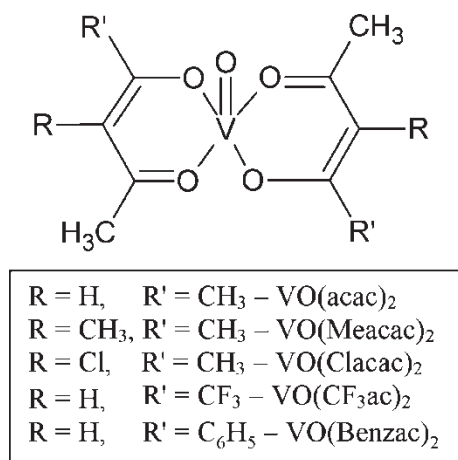| R = H,   R' = CH₃ – VO(acac)₂ |
| R = CH₃, R' = CH₃ – VO(Meacac)₂ |
| R = Cl,   R' = CH₃ – VO(Clacac)₂ |
| R = H,   R' = CF₃ – VO(CF₃ac)₂ |
| R = H,   R' = C₆H₅ – VO(Benzac)₂ |

Figure 1. Substituted VO(β-diketone)₂ complexes: VO(acac)₂, bis(acetylacetonato)oxovanadium(IV); VO(Meacac)₂, bis(3-methylacetylacetonato)oxovanadium(IV); VO(Clacac)₂, bis(3-chloroacetylacetonato)oxovanadium(IV); VO(CF₃ac)₂, bis(1,1,1-trifluoroacetylacetonato)oxovanadium(IV); and VO(Benzac)₂, bis(benzoylacetonato)oxovanadium(IV).

increasing glucose uptake by 3T3-L1 adipocytes [16,17,18]. Katoh and co-workers demonstrated a correlation between the insulin-mimetic activity of vanadyl-hydroxythiazolethione complexes and the Hammett parameter for a substituent group on the ligand, however, very few such structure-activity relationships have been reported [19]. The ability of vanadium compounds to lower blood sugar levels has been suggested to involve inhibition of a protein tyrosine phosphatase [20], but no fundamental studies with vanadyl complexes as phosphatase inhibitors have been carried out in conjunction with theoretical charge density calculations.

In this study, the inhibition potency of a series of systematically modified vanadyl-β-diketone complexes, Figure 1, bearing substituent groups with different electron inductive properties was investigated against an alkaline phosphatase obtained from calf intestine. Calf-intestine APase is a readily available, high purity, general alkaline phosphatase that was chosen to serve as a useful reference APase for assessing the inhibition potency of vanadium-containing compounds. All compounds were tested using *para*-nitrophenylphosphate (*p*NPP) as the substrate. *Ab initio* electron density calculations for the VO(β-diketone)₂ complexes were performed and the calculated charge on the vanadyl ion was shown to correlate well with the measured inhibition constants. The results of the electron density calculations should be useful for other enzyme binding and inhibition studies involving vanadyl-β-diketone complexes.

Experimental

Materials

Alkaline phosphatase from calf intestine, obtained from Merck BioSciences, Calbiochem (enzyme purity > 90% confirmed by SDS-PAGE), was used without further

purification. N-(2-hydroxyethyl)-piperazine-N′-(3-propane sulfonic acid), HEPPS buffer, from Fisher Scientific was adjusted to pH 8.0 with 0.1 M NaOH obtained from the J. T. Baker Chemical Company. All other reagents were purchased from Aldrich Chemical Company at the highest quality available and used as received. Nanopure water from a Barnstead Nanopure Infinity Ultrapure Water System was used to prepare all solutions. A 1:10 (v:v) methanol:water solution was required for complete dissolution of complexes containing the 3-methyl-2,4-pentanedione, 3-chloro-2,4-pentanedione, benzoylacetone, 1,1,1-trifluoro-2,4-pentanedione, and 4-methyl-pyridine (4-Mepy) ligands. The vanadyl-β-diketone complexes and the 4-Mepy adducts were synthesized using slightly modified procedures from those reported in the literature [21−23], i.e. the pH of the reaction mixture was maintained below 3.0 to prevent the formation of vanadyl hydrous oxide species [24]. The modification results in lower yields, but a higher purity product. The toxicology of substituted vanadyl-β-diketone complexes has not been fully elucidated, but it is expected to be similar to the parent bis(acetylacetonato)oxovanadium(IV) complex. Although LD 50 data is not available for this compound, it is know to cause digestive and respiratory tract irritation that may result in diarrhea and pulmonary edema, respectively [25]. The intact VO(acac)₂ complex, administered as an oral dose to streptozoocin-induced rats at a concentration of 125 mg V L^{-1} and as an intraperitoneal injection at a concentration of 1.275 mg V kg^{-1} in a blood glucose lowering study, was shown to be less toxic than VOSO₄ [17].

Methods

APase assay. The kinetics of calf-intestine APase-catalyzed dephosphorylation of *para*-nitrophenyl-phosphate to form *para*-nitrophenol (*p*NP) was determined from duplicate experiments at 37°C. The reaction was monitored spectrophotometrically following the increased intensity of the strong *p*NP absorption band at 405 nm. Absorbance data for *p*NP was obtained with a Bio Tek EL808 fixed wavelength, multi-channel, microplate reader using polystyrene, 96 well, assay plates with a well volume of 300 μL. Reaction mixtures consisted of 2.2 ng of calf-intestine alkaline phosphatase, 0.5 mg mL^{-1} bovine serum albumin (BSA), 30 mM HEPPS buffer (pH = 8.0), and 5 mM MgCl₂. All reaction components were pre-incubated in the wells of an assay plate for 5 minutes. The reaction was initiated by the addition of *p*NPP, which resulted in a final solution concentration between 5-4000 μM in *p*NPP. The reaction was followed for 10−20 minutes with triplicate measurements made for each substrate concentration.

Activation energy, E$_a$. The activation energy for calf-intestine APase-catalyzed dephosphorylation of 4.0 mM

RIGHTS LINK()

*p*NPP was determined from duplicate measurements of rate constants in the 20-50°C temperature range. The E_a value was used to calculate the activation free energy, enthalpy, and entropy for the APase-catalyzed reaction.

Enzyme kinetics and inhibition. Kinetic studies with VO(β-diketone)$_2$ complexes were conducted at 37°C following the procedure described above with 0.0– 10 µM inhibitor present in the pre-equilibrated reaction mixture. To obtain substrate saturation curves, the slopes obtained from change in absorbance vs. time curves were plotted as initial velocity normalized by the enzyme concentration (ν) expressed in s^{-1} vs. *p*NPP concentration (S), which ranged from 5–4000 µM. Plots of product concentration vs. time were linear for > 20 minutes ruling out product inhibition. The kinetic constants, k_{cat} and K_m, were acquired by fitting the data to the hyperbolic equation: $\nu = (k_{cat})(S)/(K_m + S)$, with a non-linear least square formula using the program Origin^{TM} 7.5. The dissociation constant of the enzyme-inhibitor complex (K_i) was calculated by fitting the data of several saturation curves in the presence of different inhibitor concentrations (I) to the general equation of the competitive inhibition model: $\nu = [(k_{cat})(S)]/[S + (K_m)(1 + I/K_i)]$. In this case, the fitting of the data to an equation with two variables (S, I) was performed using a non-linear least squares regression of the Gauss-Newton algorithm with optional damping with an *ad hoc* program written in C language [26]. The standard deviation of the parameters was also obtained using that algorithm. Values of K_i obtained by linear regression of the plots K'_m (apparent K_m) versus I using the equation $K'_m = (K_m)(1 + I/K_i)$ were not significantly different from those obtained by the former procedure. Duplicate experiments using VOSO$_4$ and Na$_3$VO$_4$ were run under identical conditions.

Calf-intestine APase has been reported to be a half-site enzyme that follows Michaelis-Menten kinetics [5]. In this investigation, the results obtained demonstrated a small negative cooperativity. Consequently, the kinetic parameters for all inhibitors were also acquired from a fit of the data to the equation: $\nu = (k_{cat})(S^n)/[S^n + (K_m(1 + I/K_i))^n]$. An average n value of $0.90 \pm .05$ was obtained using this equation, but the k_{cat}, K_m, and K_i values remain within experimental error of the values obtained by fitting the data to the Michaelis-Menten equation.

An earlier study indicated that VO(acac)$_2$ may interact with BSA [16]. Consequently, parallel inhibition studies were conducted in the presence and absence of BSA. Results indicate that BSA does not interfere with the inhibition measurements. VO(acac)$_2$, VO(Clacac)$_2$, and VO(Benzac)$_2$ were reported to maintain their integrity in solution whereas VO(Meacac)$_2$ is immediately oxidized to a vanadium(V) species [18]. UV-visible spectral data for the

VO(β-diketone)$_2$ complexes used in the present study were obtained on a Hewlett-Packard model 8453 spectrophotometer. The first three complexes and VO(CF$_3$ac)$_2$ were observed to resist oxidation and dissociation to free VO^{2+}(aq) under assay conditions for the data collection period, VO(Meacac)$_2$ was immediately oxidized.

Computational. Geometries, electronic structures, and vibrational frequencies for the VO(Meacac)$_2$, VO(acac)$_2$, VO(Benzac)$_2$, VO(Clacac)$_2$, and VO(CF$_3$ ac)$_2$ complexes, with idealized C_{2v} symmetry, were calculated using the B3LYP/6-31G(d) density-functional method, in which Becke's three-parameter hybrid exchange functional (B3) is combined with the correlation-functional of Lee, Yang and Parr (LYP) [27,28]. The functionals were operating on the electron density, which was expanded using the 6-31G(d) polarized split-valence basis set. The effect of an aqueous environment on the calculated charge distribution was modeled using an integral equation formalism version of the polarized continuum model [29]. The calculated frequencies were obtained at the scaled B3LYP/6-31G(d) level using a scaling factor of 0.963 [30] All quantum chemical calculations were carried out using the Gaussian 03 program[31].

Results and discussion

Calf-intestine APase-catalyzed dephosphorylation of *para*-nitrophenylphosphate to *para*-nitrophenol and inorganic phosphate was investigated at pH 8.0, Equation (1).

$$p\text{NPP}^{2-}(aq) + H_2O(aq) \xrightarrow{\text{C–IAPase}} \text{PO}_4^{3-}(aq)$$

$$+ p\text{NP}(aq) + H^+(aq) \qquad (1)$$
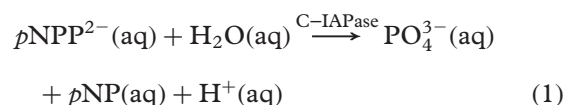
The kinetic constants calculated for this reaction are $k_{cat} = 905 \pm 11 \text{ s}^{-1}$, $K_m = 37.7 \pm 2.2 \text{ µM}$ and specificity constant $k_{cat}/K_m = 2.40 \times 10^7 \text{ M}^{-1}\text{s}^{-1}$ at 37°C. The temperature dependence of the rate constant at pH 8.0 in the 20-50°C temperature range is plotted in two ways in Figure 2, i.e. k_{cat} versus absolute temperature (T) and ln k_{cat} versus $1/T$, insert. The curve in Figure 2 was fit to the equation $k_{cat} = Ae^{(-Ea/RT)}$, using Origin© 7.5, where A = $(2.97 \pm 1.65) \times 10^7 \text{ s}^{-1}$ and $E_a = 27.0 \pm 1.0 \text{ kJ mol}^{-1}$, which is similar to that reported previously (28.0 kJ mol^{-1}) [5].

Eyring's absolute reaction-rate theory was used to convert E_a to activation free energy, $\Delta G_{cat}^{\ddagger}$, enthalpy, $\Delta H_{cat}^{\ddagger}$, and entropy, $\Delta S_{cat}^{\ddagger}$, for the reaction at 25°C [32]. The calculated values are 57.4 kJ mol^{-1}, 24.5 kJ mol^{-1}, and $-110 \text{ J mol}^{-1}\text{K}^{-1}$, respectively. These activation parameters are close to the values reported for bovine-kidney APase-catalyzed dephosphorylation of *p*NPP at pH 10.0, where its specific activity is similar to that of calf-intestine APase at pH
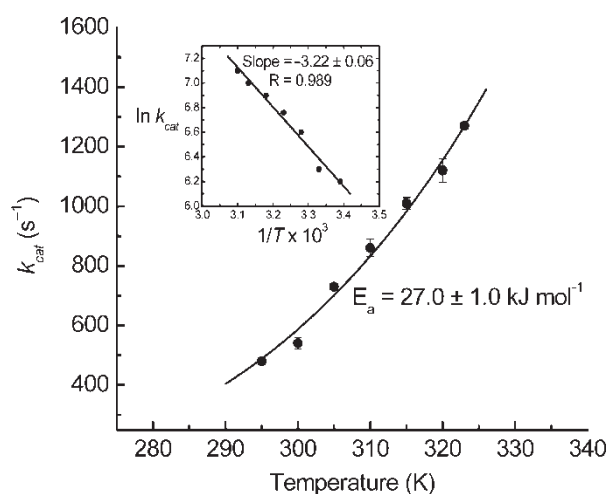
Figure 2. Temperature dependence of k_{cat} for calf-intestine APase catalyzed pNPP dephosphorylation.

8.0 [33]. The large negative $\Delta S^{\ddagger}_{cat}$ suggests substrate binding as the rate determining step, but this simple interpretation must be viewed with caution.

Inhibition of calf-intestine APase-catalyzed dephosphorylation of pNPP was carried out with a series of systematically modified vanadyl-β-diketone complexes, Figure 1. Within this series of complexes, the electron density at the vanadyl ion was varied by introducing groups with different electron-inductive properties on the β-diketone ligand. The 4-methyl-pyridine adducts of VO(acac)$_2$ and VO(Clacac)$_2$ were used to assess the role of an available coordination site on a complex's equilibrium inhibition constant, K_i. The presence of an inhibitor increases K_m but does not change k_{cat}, Figure 3. All of the complexes tested demonstrate this type of competitive inhibition behavior. This is in contrast to inhibition by phosphate, where the inhibition is "mixed" in the sense that both K_m and V (activity *sic* k_{cat}) are affected,
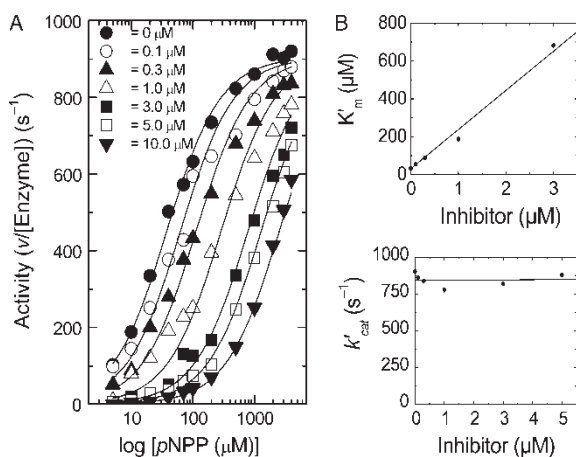

Figure 3. Panel A. Plot of APase activity versus pNPP concentration at different VO(Clacac)$_2$ inhibitor concentrations. Panel B. Plots of k'_{cat} versus inhibitor concentration and K'_m versus inhibitor concentration.

Table I. K_i values for inhibitors against calf-intestine APase at pH 8 and 37°C.

Compound	K_i (μM)
VO(CF$_3$ac)$_2$	0.07 ± 0.01
VO(Clacac)$_2$	0.15 ± 0.01
VO(Meacac)$_2$⋆	0.34 ± 0.04
VO(Benzac)$_2$	0.40 ± 0.05
VO(acac)$_2$	0.43 ± 0.04
Na$_3$VO$_4$	0.49 ± 0.04
VOSO$_4$	0.55 ± 0.06
VO(acac)$_2$·4-Mepy	0.69 ± 0.04
VO(Clacac)$_2$·4-Mepy	1.04 ± 0.13

⋆ Oxidizes to vanadium(V), possibly [VO(Meacac)$_2$]$^+$.

but competitive inhibition is still the most important component [10].

The K_i values indicate that VO(β-diketone)$_2$ complexes are stronger inhibitors than simple vanadium salts, Table I. The data suggests that inhibition increases with the positive character of a metal center. VO(CF$_3$ac)$_2$, the complex with the most electron-withdrawing substituted-β-diketone, Table II, is the most potent APase inhibitor, while complexes with less electron-withdrawing β-diketones, e.g. VO(Benzac)$_2$ and VO(acac)$_2$, are less potent inhibitors.

The inhibition constants correlate well with the results of electron density calculations, Figure 4, R = 0.995. Table II shows that VO(CF$_3$ac)$_2$ has the most positive character while the vanadyl groups of VO(acac)$_2$ and VO(Benzac)$_2$ have identical positive charges in solution. The small variation in the calculated VO positive charges is consistent with the narrow range of K_i values observed. The calculated and observed VO stretching frequencies and the calculated V—O bond distances are also consistent with the trend in the calculated VO charges. While the calculated charges on the VO groups are fairly similar, the differences are large enough to affect the aqueous solution chemistry of the complexes as well as their inhibition potency. The correlation between K_i and the positive charge on the vanadyl group suggests that a nucleophile at an enzyme active site might be directly bound to vanadium in an APase-VO(β-diketone)$_2$ inhibitor complex. This would be analogous to the situation observed in the crystal structure for *E. coli* APase in the presence of vanadate ion [12].

The inhibition kinetics of calf-intestine APase (~15% pure) with inorganic phosphate is reported to be very pH dependent, having the greatest inhibition at about pH 8 with weaker inhibition at higher pH [10]. The K_i for PO$_4^{3-}$, 1.4 μM at pH 8 [10], is ~3 times the value obtained for VO$_4^{3-}$ in the present study. Calf-intestine APase is a general phosphatase that does not utilize a strong steric mechanism of substrate selectivity and a narrow range of K_i values was expected. (The observed variation in K_i for the complexes in Table I is ~10.) A wider range

Table II.   Variations in physical properties of VO(β-diketone)$_2$ complexes.

| Compound | VO charge (au)[a] | | V=O bond length (Å) | IR: ν(V=O)(cm^{-1})[b] | | χ_G (Pauling)[c] |
	gas	soln.		calc.	obs.	
VO(Meacac)$_2$	0.733	0.672	1.572	1072	997	2.30 (CH$_3$)
VO(acac)$_2$	0.745	0.691	1.570	1076	997	2.20 (H)
VO(Benzac)$_2$[d]	0.750	0.691	1.571	1074	997	2.58 (C$_6$H$_5$)[f]
VO(Clacac)$_2$	0.770	0.733	1.568	1080	1048	3.16 (Cl)
VO(CF$_3$ac)$_2$[d]	0.783	0.752	1.565	1086	1056	3.32 (CF$_3$)[f]

[a] Mulliken charge in atomic units (au) on the vanadyl group in the gas-phase and aqueous solution; [b] V=O bond stretching frequency. The calculated frequencies were obtained using a scaling factor of 0.963. The experimental frequencies were obtained from the infrared spectra of polycrystalline samples run as nujol mulls with air as the background; [c] Pauling group electronegativity for substituents (R or R′) of Figure 1. [34]; [d] Trans configuration.

of values, however, is anticipated for these vanadyl-β-diketone complexes with specific phosphatases, e.g. a protein tyrosine phosphatase.

In some instances, vanadium complexes act as better *in vivo* inhibitors than inorganic sources of vanadium because the greater lipophilicity of the complex allows for better cell membrane permeability [13]. Significantly stronger inhibition by some of the vanadyl-β-diketone complexes was not observed in the *in vitro* studies reported here, e.g. inhibition by Na$_3$VO$_4$ is similar to VO(acac)$_2$, Table I.

Absorption spectroscopy was used to study the vanadyl-β-diketone complexes under assay conditions. The solution spectra of VO(acac)$_2$, VO(Benzac)$_2$, and VO(CF$_3$ac)$_2$ were unchanged after 30 minutes, while the spectrum of VO(Clacac)$_2$ changed slightly after 15 minutes, indicating some dissociation to a partially intact complex with a large amount of the intact complex still present. For measurements involving VO(Clacac)$_2$, the *p*NPP dephosphorylation was only followed for 10 minutes to ensure that the complex

Figure 4.   Correlation of K$_i$ (μM) for VO(β-diketone)$_2$ complexes in aqueous solution with the calculated Mulliken charge on the VO group in atomic units, R = 0.995. VO(Meacac)$_2$ oxidizes immediately to vanadium(V) under assay conditions.

remained intact for the entire data collection period. For these four compounds, the intact complexes most likely inhibit the reaction by binding to the APase through an available coordination site, i.e. the axial site occupied by water. The solution spectrum of VO(Meacac)$_2$, however, immediately changed upon dissolution indicating oxidation of the complex to a vanadium(V) species, possibly [VO(Meacac)$_2$]$^+$ [18]. Thus, the value reported in Table I for VO(Meacac)$_2$ is not a measure of the inhibition potency for the vanadium(IV) complex.

APase inhibition by an aged VO(Clacac)$_2$ solution was also investigated. After 15 minutes the solution is a slightly poorer inhibitor than the freshly prepared solution. The aged solution gradually becomes a poorer inhibitor with time, reaching a maximum K$_i$ of 1.7 μM after 4 hours. At 24 hours the aged solution has an apparent K$_i$ ($\sim$ 0.9 μM) that is 6 times greater than the freshly prepared solution.

Vanadyl-β-diketone complexes are frequently five coordinate in the solid state, but in aqueous solution the sixth coordination site is occupied by a water molecule[18]. The water molecule presumably is readily replaced in the aqua complex, providing an available coordination site on vanadium for binding the APase and eliciting inhibitory behavior. The 4-methyl-pyridine adducts of VO(acac)$_2$ and VO(Clacac)$_2$ were synthesized and the K$_i$ values measured to test this scenario. The K$_i$ value for VO(acac)$_2$·4-Mepy is higher than that for the parent VO(acac)$_2$ (0.69 μM vs. 0.43 μM), but the difference is not as dramatic as the difference between VO(Clacac)$_2$ (K$_i$ = 0.15 μM) and its 4-Mepy adduct (K$_i$ = 1.04 μM). The stronger Lewis acidity of VO(Clacac)$_2$ would provide tighter binding of the 4-Mepy ligand, which more effectively blocks APase coordination at the sixth coordination site. With a less readily available sixth coordination site, the inhibition potency of VO(Clacac)$_2$·4-Mepy is diminished to become the least effective APase inhibitor tested. VO(acac)$_2$, with weaker Lewis acidity, would not bind as tightly to a sixth ligand and the 4-Mepy ligand undoubtedly would be more readily replaced in the VO(acac)$_2$·4-Mepy adduct.
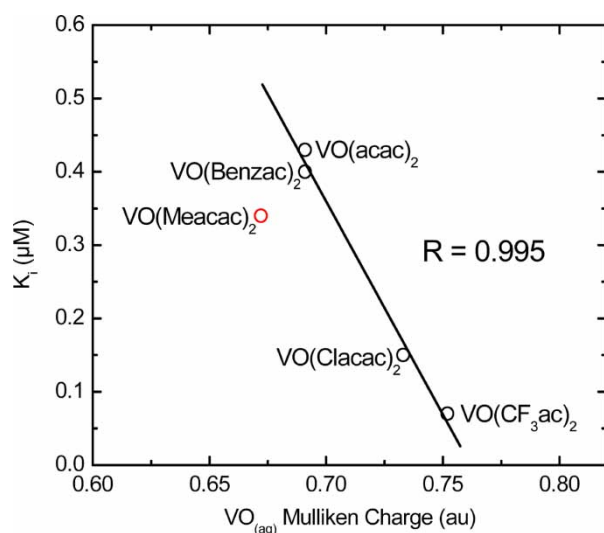
The crystal structure of vanadate bound to *E. coli* APase shows a serine nucleophile occupying an axial position in vanadium's inner coordination sphere [12]. Observation of this interaction affords the strong likelihood that vanadyl complexes bind to phosphatases in a similar fashion, i.e. through an available coordination site. It further supports the suggestion that a more positive center allows the complex to bind more tightly to the enzyme as indicated by the stronger inhibition potency of VO(CF$_3$ac)$_2$. While the solution chemistry of vanadium to some degree limited the range of electronic environments investigated, the range was wide enough to obtain meaningful data that enabled identification of a correlation between the positive charge on the VO group and the inhibition potency of the VO(β-diketone)$_2$ complex. This type of information, combined with the baseline data obtained for calf-intestine APase inhibition by the systematically modified vanadyl-β-diketone complexes, is essential for the rational design of potent phosphatase inhibitors. Additionally, the results of the *ab initio* electron density calculations should be useful for classical molecular simulations of inhibition of other phosphatases.

Acknowledgements

References

[1] Llinas P, Masella M, Stigbrand T, Menez A, Stura EA, Le Du MH. Structural studies of human alkaline phosphatase in complex with strontium: Implication for its secondary effect in bones. Pro Sci 2006;15:1691–1700.

[2] Kim EE, Wyckoff HW. Reaction mechanism of alkaline phosphatase based on crystal structures. J Mol Biol 1991;218:449–464.

[3] DeBacker M, McSweeny S, Rasmussen HB, Riise BW, Lindley P, Hough E. The 1.9 Å crystal structure of heat-labile shrimp alkaline phosphatase. J Mol Biol 2002;318:1265–1274.

[4] Le Du MH, Stigbrand T, Taussig MT, Menez A, Stura EA. Crystal structure of alkaline phosphatase from human placenta at 1.8 Å resolution. Implication for substrate specificity. J Biol Chem 2001;276:9158–9165.

[5] Chappelet-Tordo D, Fosset M, Iwatsubo M, Gache C, Lazdunski M. Intestinal alkaline phosphatase. Catalytic properties and half of the sites reactivity. Biochemistry 1974;13:1788–1795.

[6] Fosset M, Chappele D, Lazdunsk M. Intestinal alkaline-phosphatase-physical-properties and quaternary structure. Biochemistry 1974;13:1783–1788.

[7] Portmann P, Jorg A, Furrer K, Walker HS, Leuthard P, Sudan JF, Perriard F, Comment JF, Leva G, Nell JP. Calf intestinal alkaline-phosphatase .1. Improved isolation method and molar composition of the purified phosphatase. Helv Chim Acta 1982;65:2668–2681.

[8] Miggiano GAD, Mordente A, Martorana GE, Castelli A. Modification of arginine residues in calf intestinal alkaline-phosphatase. Ital J Biochem 1985;34:364–372.

[9] Schmidt G, Thannhauser SJ. Intestinal phosphatase. J Biol Chem 1943;149:369–385.

[10] Fernley HN, Walker PG. Studies on alkaline phosphatase. Inhibition by phosphate derivatives and the substrate specificity. Biochem J 1967;104:1011–1018.

[11] Ensinger HA, Pauly HE, Pfleiderer G, Stiefel T. Role of Zn(II) in calf intestinal alkaline-phosphatase studied by influence of chelating-agents and chemical modification of histidine residues. Biochim et Biophy Acta 1978;527:432–441.

[12] Holtz KM, Stec B, Kantrowitz ER. A model of the transition state in alkaline phosphatase reaction. J Biol Chem 1999;274:8351–8354.

[13] Crans DC, Keramidas AD, Drouza C. Organic vanadium compounds – transition state analogy with organic phosphorus compounds. Phosphorus Sulfur Silicon 1996;109–110:245–248.

[14] Sakurai H, Katoh A, Yoshikawa Y. Chemistry and biochemistry of insulin-mimetic vanadium and zinc complexes. Trial for treatment of diabetes mellitus. Bull Chem Soc Jpn 2006;79:1645–1664.

[15] Crans DC, Smee JJ, Gaidamauskas E, Yang L. The chemistry and biochemistry of vanadium and the biological activities exerted by vanadium compounds. Chem Rev 2004;104:849–902.

[16] Makinen MW, Brady MJ. Structural origins of insulin-mimetic activity of bis(acetylacetonate)oxovanadium(IV). J Biol Chem 2002;277:12215–12220.

[17] Reul BA, Amin SS, Buchet JP, Ongemba LN, Crans DC, Brichard SM. Effects of vanadium complexes with organic ligands on glucose metabolism: A comparison study in diabetic rats. Brit J Pharm 1999;126:467–477.

[18] Amin SS, Cryer K, Zhang B, Dutta SK, Eaton SS, Anderson OP, Miller SM, Reul BA, Brichard SM, Crans DC. Chemistry and insulin-mimetic properties of bis(acetylacetonate)oxovanadium(IV) and derivatives. Inorg Chem 2000;39:404–416.

[19] Katoh A, Yamaguchi M, Saito R, Adachi Y, Sakurai H. Insulinomimetic vanadyl-hydroxythiazolethione complexes with VO(S$_2$O$_2$) coordination mode: The correlation between the activity and Hammett's substituent constant. Chem Lett 2004;33:1274–1275.

[20] Byon JCH, Kusari AB, Kusari J. Protein-tyrosine phosphatase-1B acts as a negative regulator of insulin signal transduction. Mol Cell Biochem 1998;182:101–108.

[21] Jones MM. Some vanadyl complexes with β-diketones. J Amer Chem Soc 1954;76:5995–5997.

[22] Odunola OA, Woods JAO. Synthesis, electronic, and magnetic properties of some 3-substituted 2, 4-pentanedionatooxovanadium(IV) complexes and their 4-methylpyridine adducts. Synth React Inorg Metal-Org Chem 2001;31:1297–1310.

[23] Dodge RP, Templeton DH, Zalkin A. Crystal structure of vanadyl bisacetylacetonate: Geometry of vanadium in fivefold coordination. J Chem Phys 1961;35:55–67.

[24] Crans DC, Tracey AS. The chemistry of vanadium in aqueous and non-aqueous solution. In: Tracey AS, Crans DC, editors. Vanadium compounds: Chemistry, biochemistry, and therapeutic applications., Vol 711 USA: Oxford University Press; 1998. p 11.

[25] MSDS online, p 94 [Internet]., Vanadyl(IV)-Acetylacetonate, Acros Organic N.V., Fair Lawn, NJ. 2007 Apr 4 - [cited 2007 Oct 31]; Available from: http://www.msdsonline.com

[26] Fraser RDB, Susuki E In: Leach SJ, editor. Physical principles and techniques of protein chemistry. Part C New York: Academic Press; 1973; 301–355.

[27] Becke AD. Density-functional thermochemistry. III. The role of exact exchange. J Chem Phys 1993;98:5648–5652.

[28] Lee C, Yang W, Parr RG. Development of the Colle-Salvetti correlation-energy formula into a functional of the electron density. Phys Rev B 1988;37:785–789.

[29] Mennucci B, Cances E, Tomasi J. Evaluation of solvent effects in isotropic and anisotropic dielectrics and in ionic solutions with a unified integral equation method: Theoretical bases, computational implementation, and numerical applications. J Phys Chem B 1997;101:10506–10517.

[30] Rauhut G, Pulay P. Transferable scaling factors for density functional derived vibrational force fields. J Phys Chem 1995; 99:3093–3100.

[31] Gaussian03. Revision C.02. Wallingford, CT: Gaussian Inc. 2004.

[32] Daniels F, Alberty RA. Physical chemistry. 2nd ed. New York: Wiley and Sons Inc. 1961; 649–652.

[33] Cathala G, Brunel C, Chappelet-Tordo D, Lazdunski M. Bovine kidney alkaline phosphatase catalytic properties, subunit interactions in the catalytic process, and mechanism of Mg^{2+} stimulation. J Biol Chem 1975;250:6046–6053.

[34] Huheey JE. Inorganic chemistry. 3rd ed. New York: Harper and Row; 1983. p 156.